Liquid Crystals
Publication details, including instructions for authors and subscription information:
http://www.informaworld.com/smpp/title~content=t713926090

Optical studies on two tilted smectic phases of meta-substituted three-ring liquid crystal compounds

S. T. Wang[a]; S. L. Wang[a]; X. F. Han[a]; Z. Q. Liu[a]; S. Findeisen[b]; W. Weissflog[b]; C. C. Huang[a]
[a] School of Physics and Astronomy, University of Minnesota, Minneapolis, MN 55455, USA [b] Institut für Physikalische Chemie, Martin-Luther-Universität Halle-Wittenberg, D-06108 Halle, Germany

To cite this Article Wang, S. T. , Wang, S. L. , Han, X. F. , Liu, Z. Q. , Findeisen, S. , Weissflog, W. and Huang, C. C.(2005) 'Optical studies on two tilted smectic phases of meta-substituted three-ring liquid crystal compounds', Liquid Crystals, 32: 5, 609 — 617
To link to this Article: DOI: 10.1080/02678290500116896
URL: http://dx.doi.org/10.1080/02678290500116896

Liquid Crystals, Vol. 32, No. 5, May 2005, 609–617

Optical studies on two tilted smectic phases of meta-substituted three-ring liquid crystal compounds

S. T. WANG†, S. L. WANG†, X. F. HAN†, Z. Q. LIU†, S. FINDEISEN‡, W. WEISSFLOG‡ and C. C. HUANG*†

†School of Physics and Astronomy, University of Minnesota, Minneapolis, MN 55455, USA

‡Institut für Physikalische Chemie, Martin-Luther-Universität Halle-Wittenberg, Mühlpforte 1, D-06108 Halle, Germany

(*Received 14 August 2004; in final form 10 January 2005; accepted 13 January 2005*)

Null transmission ellipsometry and depolarized reflected light microscopy have been performed on freestanding films of two achiral meta-substituted three-ring compounds. These compounds exhibit two different tilted smectic phases, SmC_1 and SmC_2. Our studies confirmed previous results obtained from another achiral meta-substituted three-ring compound that the SmC_1 and SmC_2 phases are SmC and SmC_A, respectively.

1. Introduction

Ferroelectricity (FE) and antiferroelectricity (AFE) have been confirmed in SmC* [1] and SmC_A* phases, respectively, for many years [2, 3]. These tilted smectic phases are characterized by a stack of two-dimensional liquid layers formed by almost rod-like molecules. It was generally believed that the building block molecules must be chiral so that mirror symmetry is broken and FE and/or AFE in such systems can be allowed. However, recently, a packing order of achiral bent-core molecules in the smectic layer, which can generate a spontaneous polarization ($\mathbf{P}_{fe}$), was found by Link *et al.* [4]. Because of the tilt of the molecular long axes, domains with different handedness or racemic domains with different properties can form in the B_2 phase [4]. This intriguing discovery reveals that specific molecular packing order can yield FE and/or AFE in the phases formed by achiral molecules.

Much research has been focused on the liquid crystalline phases of bent-core molecules, since most of the achiral compounds in which mesophases showing FE and/or AFE have been found take this molecular shape [5, 6]. The chemical structure of such molecules consists of a rigid bent core with five or more aromatic rings. It is important to identify achiral molecules with a minimum number of aromatic rings, which yield bulk FE and/or AFE behaviour. Recently two groups reported observations of FE and chirality in achiral meta-substituted three-ring mesogens [7, 8]. Hird *et al.* studied bulk samples; they proposed that the observed chirality may originate from two conformations having mirror symmetry with respect to each other. However, experimental details were not given. Stannarius *et al.* performed experiments on thick freestanding films of the liquid crystal 15gt, whose chemical structure is shown in figure 1 (*a*). They suggested that in the symmetry of the phases it is more similar to bent-core compounds than to conventional rod-like molecules. However, these speculations are inconclusive. Our group also conducted detailed optical studies on the compound 15gt, but no evidence was found to support the proposal that the tilted smectic phases in the hockey-stick shaped compound are FE and chiral [9]. Thus it remains an important issue to characterize the properties of other hockey-stick shaped molecules and to determine whether they possess the properties of rod-like or bent-core molecules.

Two more hockey-stick shaped compounds, sf-35 and sf-7, have been synthesized and studied. The results found from the tilted smectic phases in both compounds are quite similar. In this paper, we report null transmission ellipsometry (NTE) and depolarized reflected light microscopy (DRLM) [10] investigations on freestanding films of compound sf-35; the results are compared with those obtained from compound 15gt. The chemical structures and phase sequences of compounds sf-35 and sf-7 are shown in figures 1 (*b*) and 1 (*c*), respectively. The transition temperatures were obtained from DSC measurements on bulk samples (for sf-35, the transition temperatures obtained from thin freestanding films are different than those acquired by DSC). The SmC_2 phase of 15gt is monotropic upon cooling. From NMR studies, the SmC_1 (SmC_2) phase is

*Corresponding author. Email: huang001@tc.umn.edu

Liquid Crystals
ISSN 0267-8292 print/ISSN 1366-5855 online © 2005 Taylor & Francis Group Ltd
http://www.tandf.co.uk/journals
DOI: 10.1080/02678290500116896

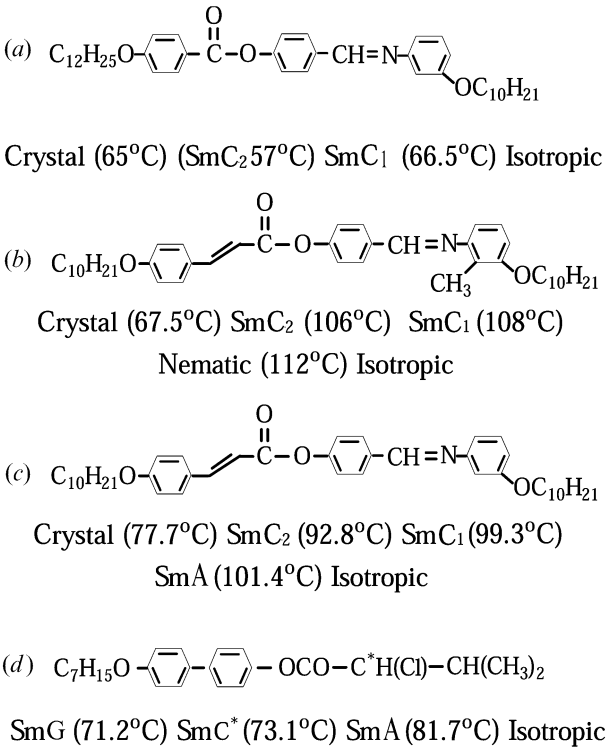

Figure 1. (a), (b), (c), and (d) show the chemical structure and bulk phase sequence for compounds 15gt, sf-35, sf-7 and A7, respectively.

found to have a SmC (SmC_A) structure [11]. Our results from these compounds confirm the synclinic and anticlinic arrangements of the SmC_1 and SmC_2 phases, respectively. Neither chirality nor response due to transverse dipole moment has been found in free-standing films of either compound. In addition, a series of surface transitions characterized by a sudden inversion of the tilt direction of a single layer [12, 13] have been observed on cooling from the SmC_1 to the SmC_2 phase for both compounds. Moreover, a layer-thinning transition has been found in compound sf-35 when the temperature is increased above the bulk SmC_1–nematic transition temperature.

2. Experimental methods

Liquid crystal freestanding films were prepared in temperature-regulated two-stage ovens filled with argon to minimize sample degradation. Each film was pulled across a circular hole in the centre of a glass cover slip in the smectic phase of the compound. In our NTE, the circular hole of diameter of 2 mm was surrounded by eight equally spaced electrodes. By applying specific sinusoidal voltages to the eight electrodes, a uniform and rotatable electric field (**E**) could be created in the plane of the film; α denotes the angle between **E** and the incident plane defined by the incident laser light and the film normal. The magnitude of the applied electric field was in the range 20–100 V cm^{-1}. In the DRLM set-up, the uniform electric field in the film plate was created by placing parallel electrodes on each side of the circular hole of diameter 4.5 mm. The magnitude of **E** was usually around 45 V cm^{-1}. By using a bipolar amplifier, a larger field, up to 10^3 V cm^{-1}, could be applied.

The details of the NTE experimental set-up have been given elsewhere [14]. If the film has net polarization in the film plane, the polarization will align with field **E**. Since **E** can be rotated through 360° in the film plane, by recording the ellipsometric parameters Δ and Ψ, as described below at each angle α, we can infer the optical symmetry of the phase and obtain the molecular arrangement in the film. Rotations of **E** were usually made with 20 equally spaced steps. NTE runs were also performed by ramping the temperature up and down. During the temperature ramp, the direction of **E** was switched between two orientations to see whether the state changed or not. In our NTE, Δ measures the phase difference between the $\hat{p}$ and $\hat{s}$ components of the incident light necessary to produce linearly polarized transmitted light. Ψ describes the polarization angle of this linearly polarized light.

Since freestanding films are used in this experimental set-up, determination of the film thickness is always the first goal. If the compound exhibits the uniaxial SmA phase without surface induced tilt, indices of refraction (n_o, n_e) and the layer thickness (d) can be determined accurately by pulling a series of films in this uniaxial SmA phase using the NTE system. At the same time, the number of layers (N) in the film can also be determined, as previously described [15]. For those compounds that do not show the uniaxial SmA phase, the number of layers in the thin films can be determined by the relationship of $\Psi \propto N^2$. In the following, we will demonstrate this relationship.

In order to simplify the argument without loss of generality, films are modelled as isotropic dielectric media with index of refraction n_2 (n_2 is about 1.5 for typical smectic phases). Propagation of the laser beam through the film is shown schematically in figure 2. In our set-up, $n_1=1$ and $\theta_1=45°$. The transmitted beam is related to the incident light through a 2×2 matrix:

$$\begin{pmatrix} E_{pt} \\ E_{st} \end{pmatrix} = \begin{pmatrix} T_{11} & T_{12} \\ T_{21} & T_{22} \end{pmatrix} \begin{pmatrix} E_{pi} \\ E_{si} \end{pmatrix} \qquad (1)$$

where E_{pi}, E_{si}, E_{pt} and E_{st} are the $\hat{p}$ and $\hat{s}$ components of the incident and transmitted light [16]. For an isotropic medium, $T_{21}=T_{12}=0$ and it can be shown that

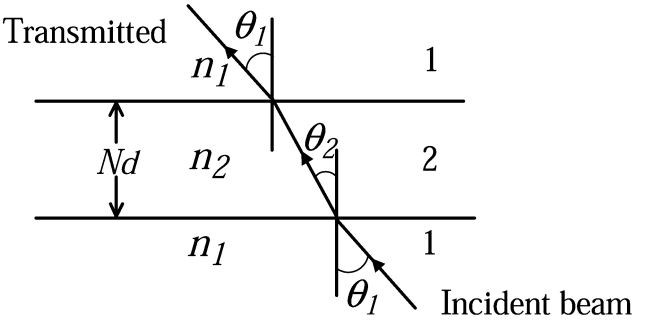

Figure 2. Schematic diagram for the propagation of the laser beam. In our set-up, $n_1=1$ and $\theta_1=45^\circ$.

$$T_{11}=\frac{4n_1n_2\cos\theta_1\cos\theta_2\exp(-i\beta)}{(n_1\cos\theta_2+n_2\cos\theta_1)^2-(n_2\cos\theta_1-n_1\cos\theta_2)^2\exp(-i2\beta)} \quad (2)$$

$$T_{22}=\frac{4n_1n_2\cos\theta_1\cos\theta_2\exp(-i\beta)}{(n_1\cos\theta_1+n_2\cos\theta_2)^2-(n_1\cos\theta_1-n_2\cos\theta_2)^2\exp(-i2\beta)} \quad (3)$$

where $\beta=2\pi n_2Nd\cos\theta_2/\lambda_o$, in which λ_o is 633 nm for our laser beam, N is the number of smectic layers and d is the layer spacing of a single layer [17]. Substituting T_{11} and T_{22} into the equations to calculate Ψ and Δ, which are given in reference [14], to the leading order term of β, we have

$$\Psi=\frac{\pi}{4}+\frac{t_1^2-t_2^2}{4t_0^2}\beta^2 \quad (4)$$

where $t_0=2n_1n_2\cos\theta_1\cos\theta_2$, $t_1={n_1}^2\cos^2\theta_1+{n_2}^2\cos^2\theta_2$ and $t_2={n_1}^2\cos^2\theta_2+{n_2}^2\cos^2\theta_1$.

From equation (4) Ψ is linear in N^2 when N is small, which is similar to the relation that reflectivity is proportional to N^2 for thin films [17]. Using this relation, the thickness of thin films can be determined by measuring Ψ and the reflectivity of different films in NTE and in DRLM, respectively. Figure 3 shows Ψ as a function of N^2 for all thin films with $N\leq10$. Although the data obtained in the SmC_1 and SmC_2 phases depend on the orientations of c-directors, its discrete nature as a function of N still allows us to determine the number of layers in thin films. In figure 3, the straight line is a linear fit to the average of Ψ of each film as a function of N^2. Our fitting result is $\Psi=45.01^\circ+0.013^\circ N^2$. Different assignments of N to the films cannot describe the data consistently. The Ψ data are also obtained from the rotation of **E**; the data are scattered so one can see that there is no detectable net polarization in the SmC_1 phase as shown below. This causes an overlap for Ψ from films which have adjacent numbers of layers, for example 8- and 9-layer films. In order to distinguish carefully two films which have adjacent numbers of layers, we cooled films to the SmC_2 phase to see whether

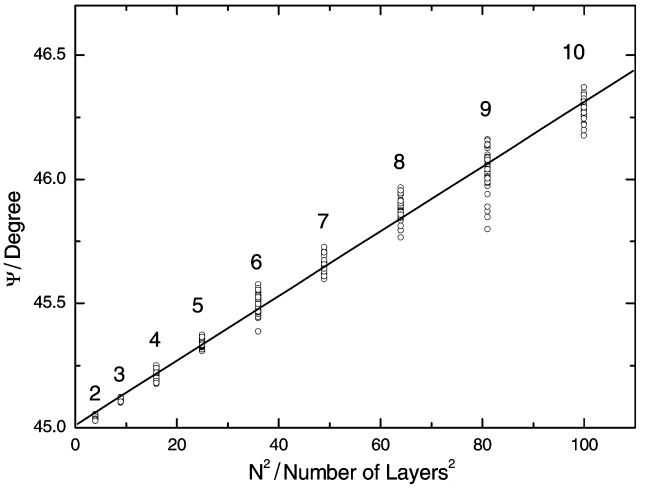

Figure 3. Ψ versus N^2 for thin films. Open circles are data and the solid line is a fit. The thickness is labelled beside the data. The data from different films were collected at various temperatures within the SmC_1 phase.

they have net polarization or not. In the lower temperature SmC_2 phase, even-layer films exhibit the polar property but odd-layer films do not. The addition of this even–odd effect allows us to assign the layer number without ambiguity.

3. Experimental results and discussion

Figure 4 shows NTE data for 2-, 3-, 4- and 5-layer films acquired at 106.8°C in the SmC_2 phase. For even-layer films (2- and 4-layer), both Δ and Ψ vary when the orientation of **E** changes; the film thus has net polarization. Δ exhibits a 180° rotational symmetry with two peaks at $\alpha=90^\circ$ and $\alpha=270^\circ$, while Ψ also displays peaks at these two angular positions. This indicates that the optical properties of the unit cell of the SmC_2 phase must have a 180° rotational symmetry and its direction of polarization is in the molecular tilt plane. For odd-layer films (3- and 5-layer), the absence of correlation between the field orientation and Δ suggests that there is no detectable net polarization. This even–odd layering behaviour indicates that the SmC_2 phase displays a SmC_A structure, and it shows results similar to another hockey-stick compound [9]. Two models may describe the origin of the net polarization. One is flexoelectric polarization due to a non-uniform tilt profile through the layers [18]; the other is longitudinal polarization due to symmetry-breaking at the surfaces [19]. While both models can describe our results satisfactorily, we choose the second to describe the results as shown in figure 4. By performing the simulation using the 4×4 matrix method [20], the anticlinic molecular arrangement in

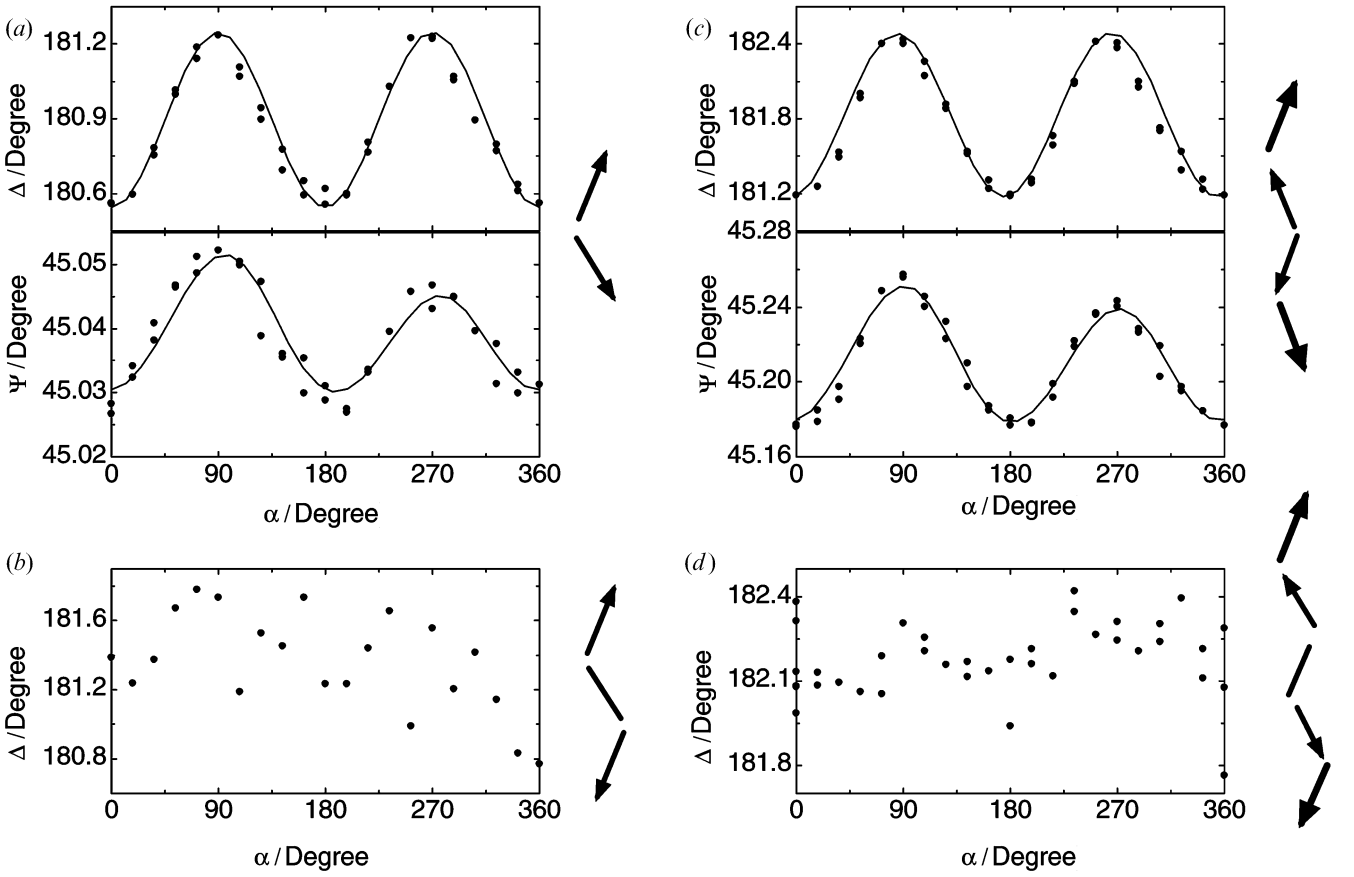

Figure 4. Δ and Ψ versus α at 106.8°C in the SmC_2 phase under $\mathbf{E}=22\,\mathrm{V\,cm^{-1}}$. Data in (*a*), (*b*), (*c*) and (*d*) are from 2-, 3-, 4- and 5-layer films, respectively. Symbols are data, and solid lines in (*a*) and (*c*) are simulation results. The cartoons beside the figures show the tilt structures. Arrows indicate the direction of longitudinal polarization; heavy arrows indicate larger polarizations at the surfaces.

the SmC_2 phase is confirmed. The simulated results are shown as the lines in figures 4(*a*) and 4(*c*). The simulation parameters of the layer spacing, tilt angle, n_e and n_o are 3.66 nm, 35°, 1.66 and 1.49, respectively; the layer spacing is determined by X-ray diffraction. Using a space-filling model, we obtained the molecular length≈4.5 nm; the tilt angle can then be obtained. Because compound sf-35 does not exhibit the uniaxial SmA phase, two indices of refraction cannot be measured using NTE as before [15]. Since several key chemical groups in the core part of sf-35 are the same as those of DOBAMBC (4-decyloxybenzylidene-4-amino-2-methylbutyl cinnamate), we used the indices of refraction of DOBAMBC in the simulation.

To address the 180° rotational symmetry of the Δ data from even-layer films as discussed above, we draw the two anticlinic molecular arrangements of a 2-layer film at $\alpha=0°$ and $\alpha=180°$, as shown in figure 5. For both configurations, the laser beam is incident on the film from the bottom and passes through layer 1 (or 1′) and then layer 2 (or 2′). Because the wavelength of the incident laser beam is much larger than the thickness of the film, layer 1 (or 2) in the first configuration, to a good approximation, is equivalent to layer 2′ (or 1′) in the second configuration and they will have the same

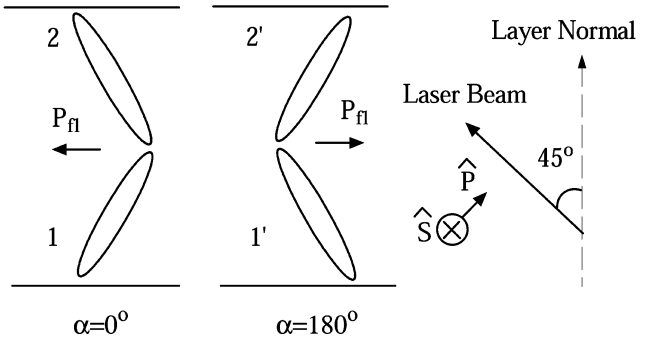

Figure 5. Two anticlinic molecular arrangements of a 2-layer film at $\alpha=0°$ and $\alpha=180°$. $\mathbf{P}_{fl}$ is the net polarization of the film.

effect on the incident laser beam.[†] Δ is the phase difference between the $\hat{p}$ and $\hat{s}$ components and the pass sequence of the laser beam through the layers will not greatly affect it; so Δ within our resolution will have a 180° rotational symmetry. On the other hand, both experimental data and simulation results show that Ψ does not have such symmetry. We still have no simple physical picture of Ψ allowing us to explain this lack of symmetry.

In the SmC_1 phase, no polarization was detected for either even- or odd-layer films in the NTE studies, except for the 2-layer films which remain in the anticlinic configuration until films rupture above 116°C (this effect is presented in figures 12 and 13). A SmC structure is expected for the SmC_1 phase. Previous studies of compound 15gt also show this behaviour [9]. In order to confirm that the SmC_1 phase really has the SmC structure, we doped a small amount (4%) of chiral compound A7 [21] into sf-35. The chemical structure and phase sequence of A7 are shown in figure 1 (*d*). The freestanding films of this chiral doped mixture could be aligned and rotated by the electric field. Since surface effects will be more dramatic on thin films than thick ones, rotation data from a thick film will be more helpful to determine the bulk SmC_1 structure. As shown in figure 6, the rotation data from a ~30-layer film of the mixture in the SmC_1 phase indicate that it has the synclinic SmC* structure [25]. (The Δ versus α curve shown in figure 6 is characteristic of a freestanding film having a synclinic, SmC*-like, molecular arrangement; such an observation is further confirmed by the simulation results.) The fitting of a SmC* structure with transverse polarization perpendicular to the tilt plane is shown as solid lines. Doping with a small amount of chiral compound lowers the SmC_1–SmC_2 phase transition temperature; however, it should not change molecular arrangements in these phases. So it is clear that the SmC_1 phase of sf-35 has a SmC-like structure.

On cooling into and heating from the SmC_2 phase, the even-layer films show behaviour different from the odd-layer films. Figure 7 shows Ψ and Δ as a function of temperature for an even-layer film (N=10). The data for an odd-layer film (N=9) are given in figure 8. As shown in figure 7, below T_3 (106.3°C), Δ_{90} is different from Δ_{180} and the 10-layer film is in the SmC_2 phase, which is polar. Above T_1 (108.3°C), the data are scattered, indicating that there is no net polarization in the film, and it may be in the SmC_1 phase. Between T_1 and T_2 (107.7°C), the film is in another polar structure which is different from the structure below T_3, since Δ_{180} between T_1 and T_2 is smaller than that below T_3. For the 9-layer film as shown in figure 8, the data in

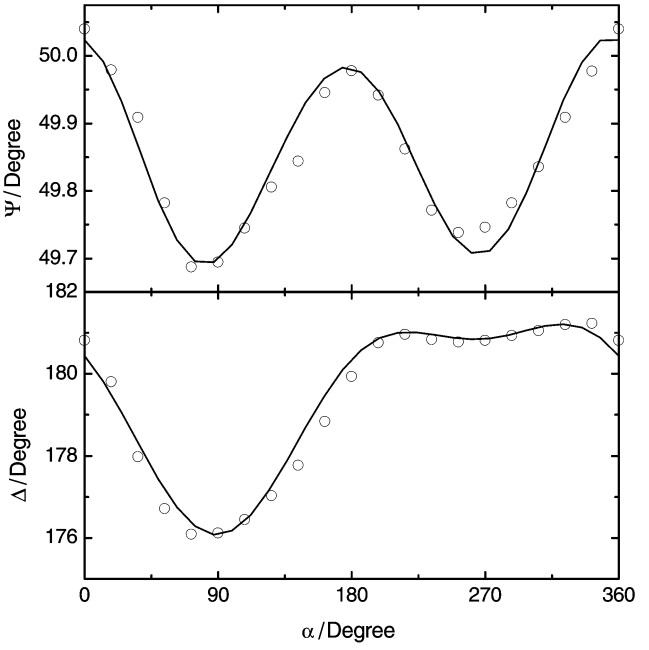

Figure 6. Δ and Ψ versus α from a ~30-layer film at 101.6°C in the SmC_1 phase of the sf-35 (4% A7) mixture. The strength of **E** is 60 V cm^{-1}. Open circles are the data and solid lines are the simulation results.

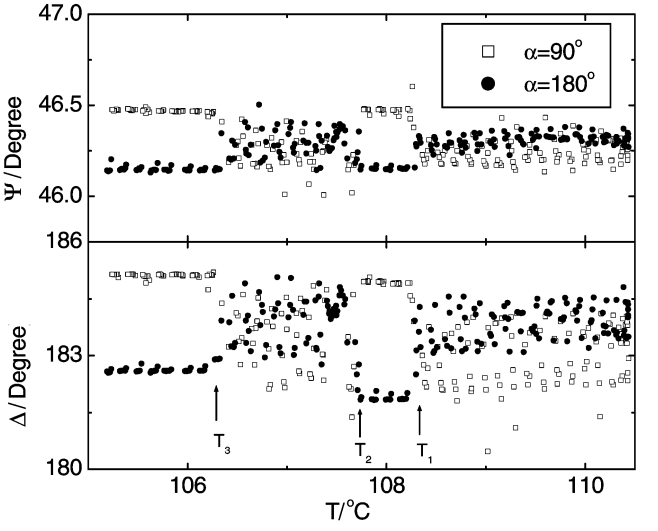

Figure 7. Temperature dependence of Ψ and Δ obtained on cooling at 20 mK min^{-1} under two electric field orientations, with **E**=27 V cm^{-1} from a 10-layer film. During cooling, the direction of **E** was switched between 90° (open squares) and 180° (solid dots) every 4 min. Three upward arrows at T_1=108.3°C, T_2=107.7°C, and T_3=106.3°C indicate three transition temperatures.

[†]In this discussion, we ignore the effect of longitudinal polarization on the laser beam.

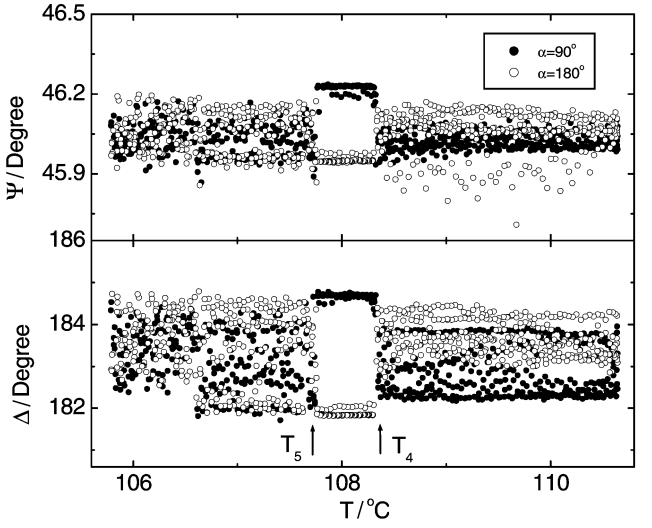

Figure 8. Temperature variation of Ψ and Δ acquired upon cooling at 5.5 mK min^{-1} under two electric field orientations, with $\mathbf{E}=27\,\mathrm{V\,cm^{-1}}$ from a 9-layer film. Open circles and solid dots are the data taken under $\alpha=180°$ and $\alpha=90°$, respectively. Two upward arrows at $T_4=108.3°C$ and $T_5=107.7°C$ indicate two transition temperatures.

the SmC_1 and SmC_2 phases are both scattered. However, there exists a temperature window around 108°C between T_4 (108.3°C) and T_5 (107.7°C) in which the 9-layer film shows a polar structure. Similar data indicating a polar structure are also observed at around the same temperature window for 7- and 8-layer films. We believe that the structure in this temperature window (around 108°C) for both even- and odd-layer films is similar. It can be seen more clearly in figure 9.

Parameters Ψ and Δ as functions of α for 10-layer and 9-layer films within polar response windows are shown in figures 9 (*a*) and 9 (*b*), respectively. In figure 9 (*a*), although Ψ values obtained at 108°C and 106°C are almost the same, the data for Δ are obviously different at these two temperatures. Δ_{180} at 108°C is smaller than that at 106°C, which is consistent with the data shown in figure 7. In addition, there is 180° rotational symmetry for the Δ data at 106°C but those at 108°C do not have such symmetry. Values of Ψ and Δ acquired at 108°C for a 9-layer film are similar to values obtained at the same temperature from a 10-layer film. This may indicate that the polar structure between T_4 and T_5 for the odd-layer film is similar to that structure between T_1 and T_2 for an even-layer film. It was confirmed by the simulation results (solid lines) obtained using the

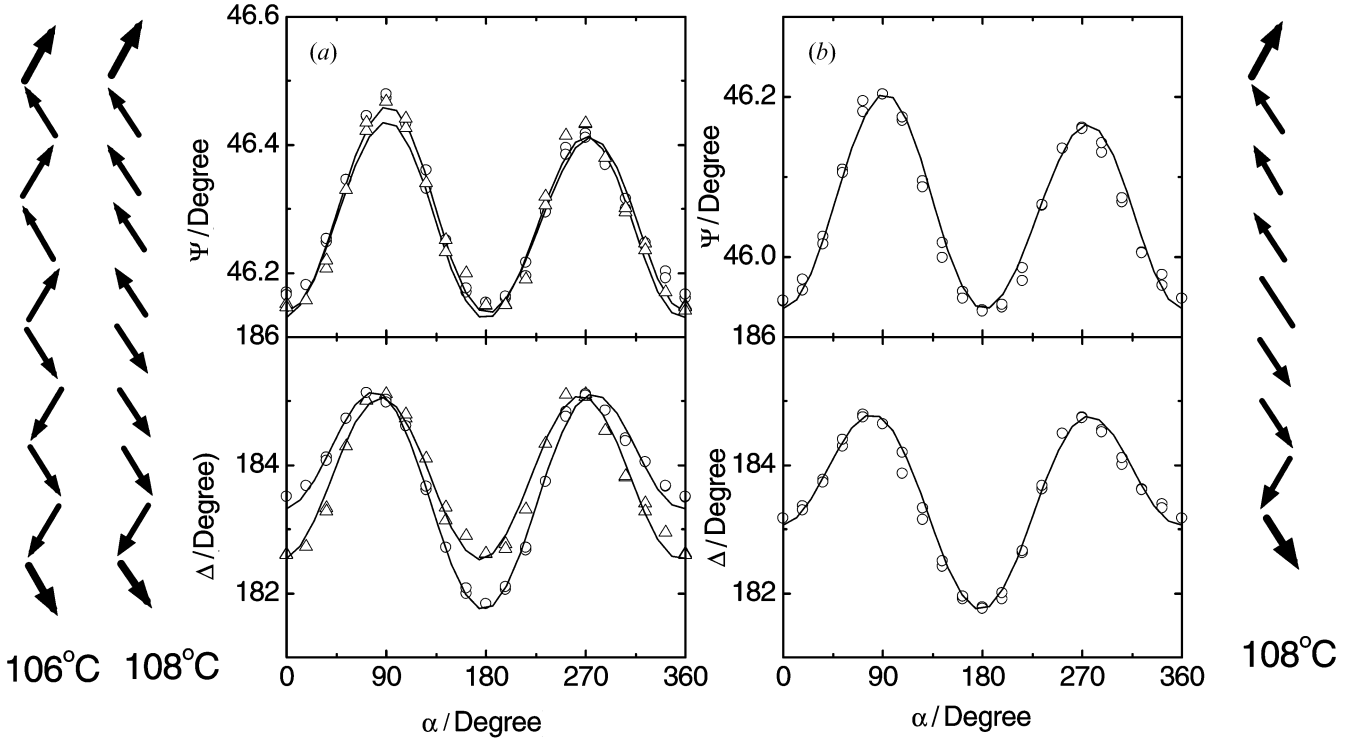

Figure 9. Ψ, Δ versus α with $\mathbf{E}=22\,\mathrm{V\,cm^{-1}}$, from (*a*) a 10-layer film and (*b*) a 9-layer film. Open circles and triangles are the data obtained at 108.0 and 106.0°C, respectively; solid lines are the simulation fits. The cartoons beside the figures show the tilted structures used in the simulation; heavy arrows indicate surface layers which have larger polarizations than interior layers.

structure shown beside figure 9. The simulation parameters of the layer spacing, n_e and n_o are the same as those used for simulating the thin films (2- and 4-layer films). (In order to fit the data of 9- and 10-layer films better, and also keep the layer spacing and two indices of refraction the same as for 2- and 4-layer films, we use the tilt angle 33° for 9- and 10-layer films instead of 35° in our simulation.)

The polar structure formed between the SmC_1 and SmC_2 phases is believed to be an intermediate structure. It can be explained by the growth of an anticlinic interface and is confirmed by the simulation of the rotation data. As shown in figure 10, Δ_{180} continuously increases and Δ_0 decreases as the layers are inverted one by one. The tilt inversion shown in the cartoon beside figure 10 starts from the surface layers. However, the tilt inversion may start from the middle layers of the film. Comparing the data and simulation results, we found that there are two layers inverted in this intermediate polar structure shown in figures 7 and 9 (*a*). However, the simulation cannot tell which two layers invert. Our previous studies on another hockey-stick compound, 15gt, demonstrated a layer-by-layer growth of anticlinic layers, which is associated with four transitions (two polar structure windows) for a 7-layer film. However, here only one polar window has been observed for both 7-layer and 9-layer films in our NTE system. The reason is probably that other polar states are not sufficiently stable, or their temperature windows are too small, to allow our system to detect the state. On decreasing or increasing the temperature, we observed several transition fronts in 7- to 10-layer films. However, they moved across the film so fast that the NTE could not catch the data from each state, since at least one minute is needed to find the appropriate positions of the analyser and polarizer that yield the minimum transmitted intensity.

DRLM was also performed on the SmC_1 and SmC_2 phases. Due to enhanced surface ordering, 2- and 4-layer films are polar in the SmC_1 temperature window, and keep the anticlinic SmC_A arrangement. Except for these two films, no net polarization was observed in all other films with different thicknesses in the SmC_1 phase. In addition, there is no evidence indicating that the SmC_1 phase is chiral. On cooling from the SmC_1 to the SmC_2 phase, a series of transitions between polar and non-polar states was observed. As an example, the images of a polar to non-polar transition in 19- and 16-layer films are shown in figure 11. On cooling to the SmC_2 phase, the films exhibited the same even–odd layering effect as observed in our NTE system.

In order to check any additional non-polar–polar transition into the nematic (or isotropic) phase window for a 10-layer film, we increased the temperature until

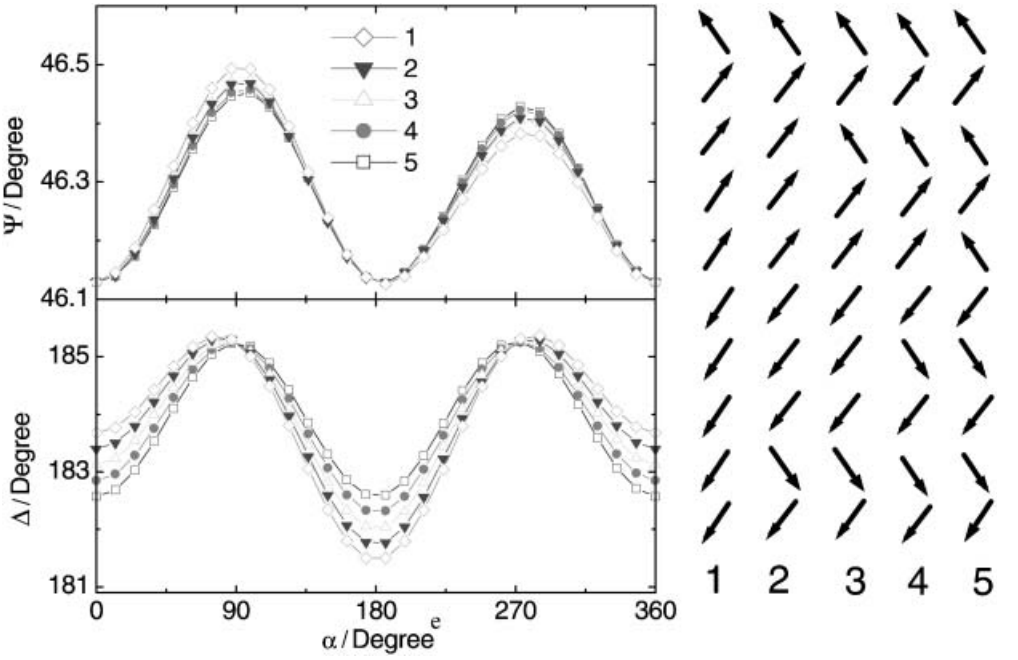

Figure 10. Simulated Ψ, Δ versus α from a 10-layer film with different structures, showing one possible scenario of the layer-by-layer tilt inversion. Open diamonds, solid triangles, open triangles, solid dots and open squares are the data simulated from structures 1, 2, 3, 4 and 5, respectively; the arrows indicate the directions of longitudinal polarization. The magnitude of polarization for each layer will decrease from the surface into interior layers.

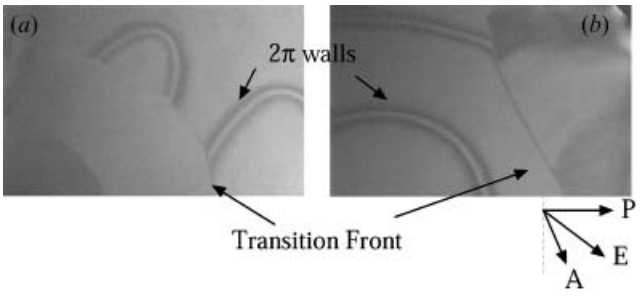

Figure 11. Video images captured at one polar–non-polar transition for (*a*) a 19-layer film and (*b*) a 16-layer film around 109°C under $\mathbf{E}=45\,\mathrm{V\,cm^{-1}}$. In the polar region, 2π walls can be seen and most *c*-directors are aligned by the electric field. In the non-polar region, there is no net polarization and the c-director does not respond to the field.

the film collapsed. To our surprise, a layer-thinning transition was observed for this compound, as shown in figure 12 [22]. The step-like change of Ψ indicates the layer-by-layer thinning of the film in the following sequence: $N=10$, 9, 8, 7, 6, 5 and 2. The discrete nature of Ψ for different films is consistent with the data in figure 3. In figure 12, the scattering data obtained from 10-layer to 5-layer films indicate that these films are in the SmC_1 phase. However, Δ_{90} and Δ_{180} for the 2-layer film are separate and different; the anticlinic SmC_A arrangement is maintained at this temperature. Values of Ψ and Δ as functions of the orientation of **E** were obtained at 118.9°C for this 2-layer film. The results are similar to those for a 2-layer film in the SmC_2 phase shown in figure 4 (*a*), confirming the 2-layer anticlinic

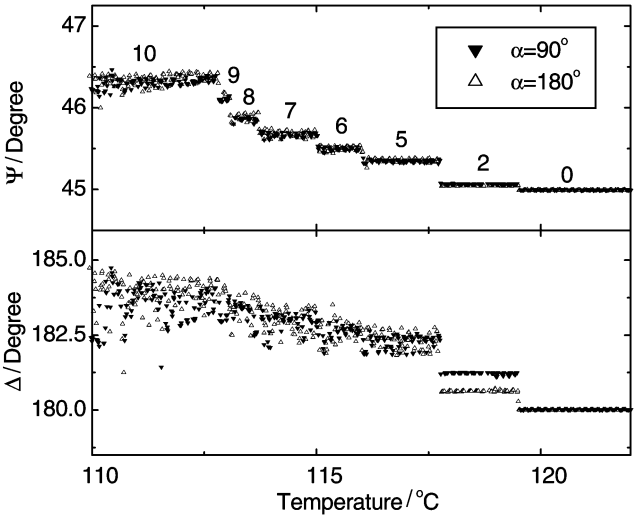

Figure 12. Ψ, Δ versus temperature on heating at $20\,\mathrm{mK\,min^{-1}}$ under two field orientations with $\mathbf{E}=22\,\mathrm{V\,cm^{-1}}$ starting from a 10-layer film. During heating, the direction of **E** was switched between 90° (solid triangles) and 180° (open triangles) every 4 min.

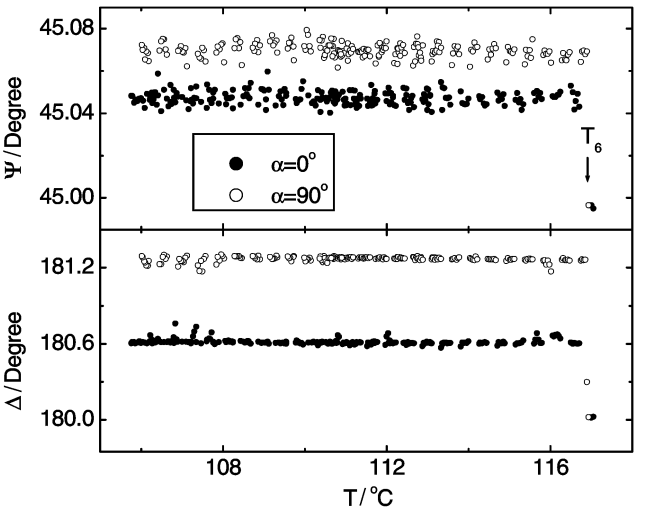

Figure 13. Temperature dependence of Ψ and Δ with $\mathbf{E}=44\,\mathrm{V\,cm^{-1}}$ for a 2-layer film. The data below 110.5°C were obtained upon cooling at $60\,\mathrm{mK\,min^{-1}}$; the data above 110.5°C were obtained on heating at $60\,\mathrm{mK\,min^{-1}}$. During heating or cooling, the direction of **E** was switched between 0° (solid dots) and 90° (open circles) every 4 min. This film collapsed at $T_6=116.8$°C.

SmC_A arrangement. Values of Ψ and Δ obtained at two different α-values as a function of temperature through a very wide temperature window are shown in figure 13. Here the 2-layer film held the anticlinic arrangement throughout until collapse. This is consistent with our DRLM observation for the 2-layer film.

It is clear that the Δ data are noisier than those for Ψ. As we know, Δ is very sensitive to the indices of refraction in the layer plane. Because the film has no net polarization, the molecules are not aligned by the electric field. The fluctuations of the *c*-directors of molecules will be large at high temperature; as the c-directors fluctuate, the in-plane indices of refraction will also fluctuate, causing scattering of the Δ data. However, Ψ is less sensitive to the indices of refraction and depends more on the thickness of the film; the Ψ data are therefore less subject to noise. Another feature is that the Ψ data shown in figure 12 are cleaner than those shown in figure 3 (see 9-layer). A possible reason is that at temperatures above the bulk nematic–isotropic transition, the *c*-directors will fluctuate more and tend to become randomly distributed about the layer normal. The film will then be close to the uniaxial phase and Ψ will be less noisy.

4. Conclusion

We have studied three different hockey-stick shaped compounds using ellipsometry and depolarized light microscopy. The results clearly demonstrate that the SmC_1 phase is an achiral SmC phase and the SmC_2 is a

SmC_A. No evidence has been found to suggest that the tilted smectic phases in the hockey-stick-shaped compounds possess chirality. In addition, simulations have been employed to demonstrate the layer-by-layer transition, and an interesting layer-thinning transition has been found in one of the compounds.

Acknowledgements

This research was supported in part by the National Science Foundation, Solid State Chemistry Program under Grant No. DMR-0106122. X.F.H. wishes to acknowledge financial support from the Stanwood Johnston Memorial Fellowship, University of Minnesota.

References

[1] R.B. Meyer, L. Liebert, I. Strzelecki, P. Keller. *J. Phys. (Paris), Lett.*, **36**, L69 (1975).
[2] M. Fukui, H. Orihara, Y. Yamada, N. Yamamoto, Y. Ishibashi. *Jpn. J. appl. Phys.*, **28**, L849 (1989).
[3] A.D.L. Chandani, Y. Ouchi, H. Takezoe, A. Fukuda, K. Terashima, K. Furukawa, A. Kishi. *Jpn. J. appl. Phys.*, **28**, L1261 (1989).
[4] D.R. Link, G. Natale, R. Shao, J.E. Maclennan, N.A. Clark, E. Körblova, D.M. Walba. *Science*, **278**, 1924 (1997).
[5] G. Pelzl, S. Diele, W. Weissflog. *Adv. Mater.*, **11**, 707 (1999).
[6] D.M. Walba, E. Körblova, R. Shao, J.E. Maclennan, D.R. Link, M.A. Glaser, N.A. Clark. *Science*, **288**, 2181 (2000).
[7] M. Hird, J.W. Goodby, N. Gough, K.J. Toyne. *J. mater. Chem.*, **11**, 2732 (2001).
[8] R. Stannarius, J. Li, W. Weissflog. *Phys. Rev. Lett.*, **90**, 025502 (2003).
[9] X.F. Han, S.T. Wang, A. Cady, Z.Q. Liu, S. Findeisen, W. Weissflog, C.C. Huang. *Phys. Rev. E*, **68**, 060701(R) (2003).
[10] R. Pindak, C.Y. Young, R.B. Meyer, N.A. Clark. *Phys. Rev. Lett.*, **45**, 1193 (1980).
[11] B. Das, S. Grande, W. Weissflog, A. Eremin, M.W. Schröder, G. Pelzl, S. Diele, H. Kresse. *Liq. Cryst.*, **30**, 529 (2003).
[12] D. Schlauf, Ch. Bahr. *Phys. Rev. E*, **57**, R1235 (1998).
[13] X.F. Han, D.A. Olson, A. Cady, J.W. Goodby, C.C. Huang. *Phys. Rev. E*, **65**, 010704(R) (2002).
[14] D.A. Olson, X.F. Han, P.M. Johnson, A. Cady, C.C. Huang. *Liq. Cryst.*, **29**, 1521 (2002).
[15] P.M. Johnson, D.A. Olson, S. Pankratz, Ch. Bahr, J.W. Goodby, C.C. Huang. *Phys. Rev. E*, **62**, 8106 (2000).
[16] M. Born, E. Wolf. *Principles of Optics*. Cambridge University Press, Cambridge (1997).
[17] C. Rosenblatt, N.M. Amer. *Appl. Phys. Lett.*, **36**, 432 (1980).
[18] R.B. Meyer. *Phys. Rev. Lett.*, **22**, 918 (1969).
[19] D.R. Link, J.E. MacLennan, N.A. Clark. *Phys. Rev. Lett.*, **77**, 2237 (1996).
[20] D.W. Berreman. *J. opt. Soc. Am.,* **62**, 502 (1972); H. Wöhler, G. Haas, M. Fritsch and D.A. Mlynski. *Opt. Soc. Am., A***5**, 1554 (1988).
[21] Ch. Bahr, G. Heppke, B. Sabaschus. *Liq. Cryst.*, **11**, 41 (1992).
[22] T. Stoebe, P. Mach, S. Grantz, C.C. Huang. *Phys. Rev. Lett.*, **73**, 1384 (1994).